ASSESSMENT OF ICE-DAM COLLAPSE BY TIME-LAPSE PHOTOS AT THE PERITO MORENO GLACIER, ARGENTINA

ABSTRACT

The present work presents a feasibility study on the implementation and performance assessment of time-lapse processing of monoscopic image sequence, acquired by calibrated camera in Perito Moreno Glacier. The glacier is located at 50° 28' 23''S, 73° 02' 10''W at the Parque Nacional Los Glaciares, South Patagonia Icefield, Santa Cruz, Argentina and has experienced minor fluctuations or unusual behavior with respect to others glaciers since early 1960's until nowadays. The objective of this study was to determine the evolution and changes in the ice-dam collapse of Perito Moreno that started on November, 23 2012 and collapse on January, 19 2013. Two pictures per day were acquired since October 2012 until February, 2013, with a total of 135 days. Image processing was supported by ground data. To obtain a robust matching a 2D affine transformation was applied to co-register them. The technique allowed determining the distortion of image pixels in the images and estimating the uncertainty of scale factor. Time-lapse gave accurate estimates for information extraction. Changes in height level of the Brazo Rico lake were validated by direct data in order to determine the degree of uncertainty in the estimation of changes in the glacier obtaining an optimal correlation. Finally, advanced values of the front of Perito Moreno, velocities of 0.67 md^{-1} ± 0.003 m approx. were determined and the tunnel evolution also.

KEY WORDS: time-lapse, information extraction, ice-dam change, Perito Moreno

1. INTRODUCTION

The changes that are occurring in regional climate affect cryospheric environments and have a direct implication on the hydrological cycle. During the late 20th and early 21st centuries, glaciers have suffered a global recession, in which has been a steady increase in the average temperature on Earth. Even when all the glaciers have a response to the clime, not all of them have the same bearing depending on many characteristics. For example, some glaciers experience advances or *unusual* dynamics respect to others. In South America, Patagonia Ice field, Argentina, there is a glacier named Perito Moreno (PM) that has had minor fluctuations since early 1960 (Aniya and Skvarca, 1992) until our days leaning against to Peninsula de Magallanes and producing an ice-dammed lake. This glacier has experienced numerous collapses since the early twentieth century. The latest development was on January 19, 2013 that experienced a new rupture of the ice-dam at the Peninsula de Magallanes.

Considering that glaciers are usually located in difficult to access areas with complex topography and extreme weather conditions, their monitoring from the ground is a rather complex task. Consequently, remote sensing, represents an attractive approach to map glaciers. Despite of the recent dominance of active sensors, optical image-based extraction by photogrammetry has seen significant improvements recently, and provides a less accurate yet very inexpensive alternative to lidar and SAR techniques.

Since the mid-nineteenth century, terrestrial photogrammetry has been become in a common use and economical technique to mapping mountain areas. The terrestrial mode is usually less accurate than aerial at the same range, but has advantages for environmental monitoring studies in rather small areas. In general, this technique in some cases is conditioned by the topography. To monitor the behavior and dynamics in a natural phenomenon, time-lapse technique allows having a good spatial and temporal resolution, e.g. daily data, and insights that have advantages over aerial mode. In cases such as glaciers with natural impoundments (ice, sediments, etc.) the technique become in a good opportunity to be implemented to monitor the environment. This technique in monosopic and stereoscopic modes has been used successfully in glaciological applications since the 90s to present day (Harrison, 1992; Hashimoto et al., 2009; Ahn and Box, 2010; Svanem, 2010, Maas et al, 2010; Rivera et al., 2012; Danielson and Sharp, 2013).

This study has the objective to work with monoscopic time-lapse images acquired by non-metric professional DSLR camera system to investigate surface deformations, velocities and evolution of the ice-dam collapse from October, 2012 until January, 2013. The system used in this work made contributions in the evaluation of the time-lapse technique and in the ice-dam dynamics derived from the glaciological topic.

1. STUDY AREA

The South Patagonia Icefield (SPI) is located in South America, Argentina and Chile, covering an area of 13,000 km^2 with an approximately 30-40 km of average width and mean altitude of 1,191 m ASL (Aniya and others, 1996). At present, the three largest reservoirs of fresh water on continental shelves, in order of importance, are Antarctica, Greenland and Patagonian Continental Ice Shelf. Perito Moreno glacier is located at 50° 28’ 23’’S, 73° 02’ 10’’W in the Parque Nacional Los Glaciares, SPI, Santa Cruz, Argentina. This is an important calving glacier in the region due its size and *unusual* behavior. The terminus of PM is divided in the Canal de los Témpanos, Lago Argentino, and Brazo Rico or Lago Rico (Figure 1).

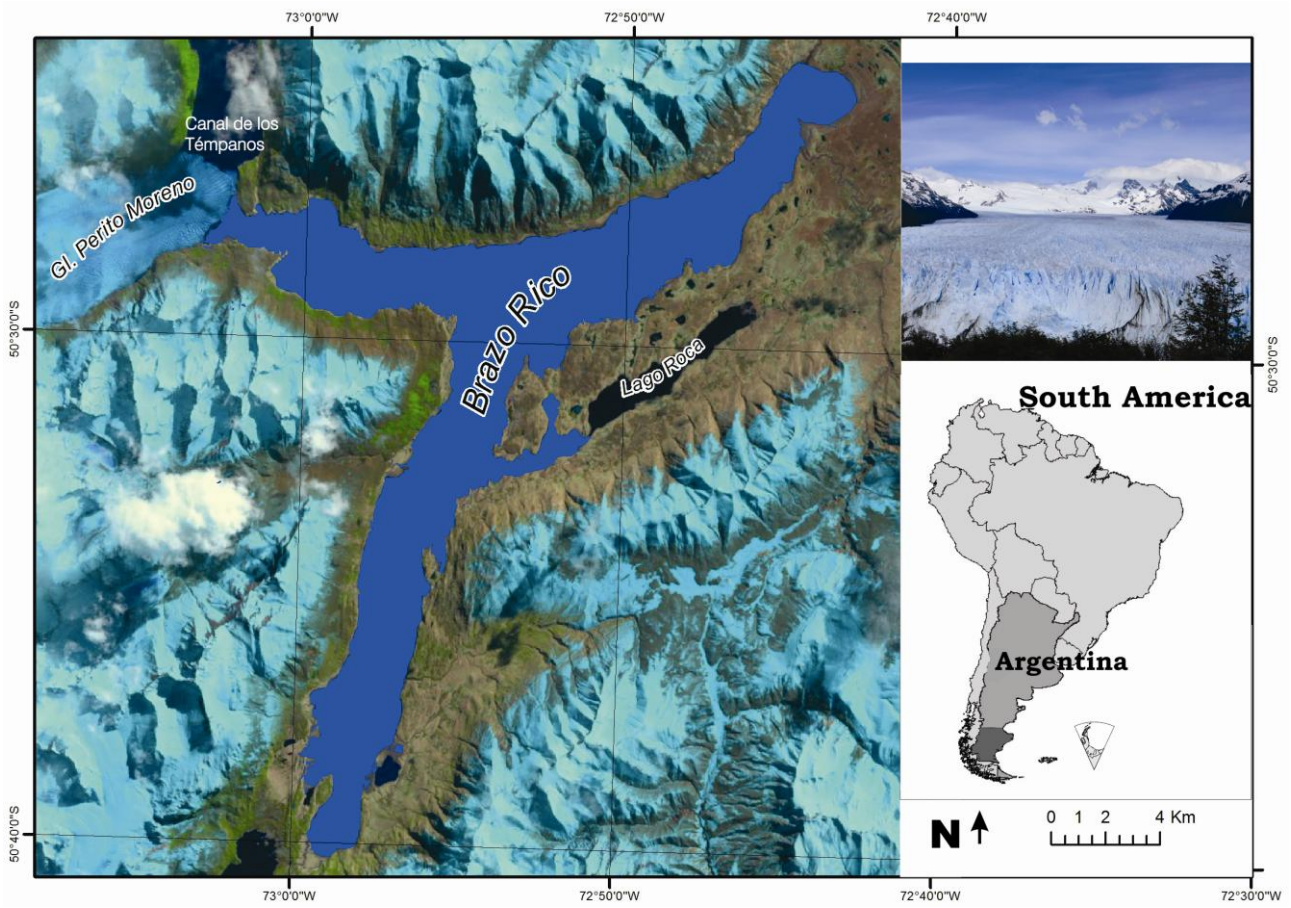

Figure 1. Map of the study area.

3. DATA & METHODS

3.1 Camera system and image collection

To support the field image acquisition, an integrated data acquisition system was built around the CANON EOS Mark II DSLR camera; pixel size: 7.2 µ, focal length: 50 mm; view angle: 46°. The camera was calibrated several times, first by USGS, and prior to field deployment. Camera calibration parameters obtained by using Photomodeler are listed in Table 1. The system is powered by two 12V/7Ah electrolyte batteries, charged by two 38W solar panels. The camera with the supporting electronical system was placed in a waterproof box. A front visor and a glass plate protect the camera from reflections and the environment. A glass plate installed in the back of the box to allow to monitor the camera status.

The image acquisition system was installed on a rigid metal structure, fixed to outcrops of the shoreline of Lake Brazo Rico. The location, chosen in accordance with National Park requirements, provides a good side view of PM, see Fig. 2. The camera gives a normal view (≅ 90°) from the base. The image acquisition started on April, 17 2012, and two pictures per day were captured at 10 am and 8 pm local time for 368 days. In this study, five months of data, from 1st of October 2012 until 12st of February 2013 was used.

Focal Length	50.425 ± 0.014 mm
Xp - principal point x	17.048 ± 0.011 mm
Yp - principal point y	11.655 ± 0.012 mm
K1 - radial distortion 1	5.953e-005 ±8.8e-007
K2 - radial distortion 2	-2.007e-008 ± 6.6e-009
K3 - radial distortion 3	0.000e+000

Table 1. Distortions coefficients

Figure 2. Systems and components of the camera.

3.2 Ground support data

Ground control points (GCPs) based on GPS surveys were established in the field, including the camera projection center. The GCPs based on using a variety of topographic features were measured, such as rocky outcrops that are assumed to be static in the proximity of the glacier. The double-frequency Trimble 5700 receiver measurements were referenced to the SGM (Station Glaciar Moreno) and SGU (Station Glaciar Upsala) CORS stations that are located at Brazo Rico lake and Upsala glacier. The computations were based on DGPS static positioning method. The results were converted to the POSGAR98 (Posicionamiento Geodésico Argentino) (Lauria, 2009) coordinate system. The data was processing on Bernese software version 5.0 (Dach et al., 2007), using fixed solutions at the 95% confidence level. The RMSEs (root-mean-square error) for the GCPs were: RMS_N = 0.001 m, RMS_E = 0.0008 m, and RMS_U = 0.0025 m; note that these numbers appear a bit too optimistic.

Also, six points on the glacier surface and three points on the outcrops (inaccessible to measured by GPS) were measured by total station surveying, using the forward intersection method from two bases correctly georeferenced by GPS. The points taken into account were pinnacles in different depths, and the objective was to obtain the altitude of the glacier. Figure 3 shows the distribution of GCPs and checkpoints.

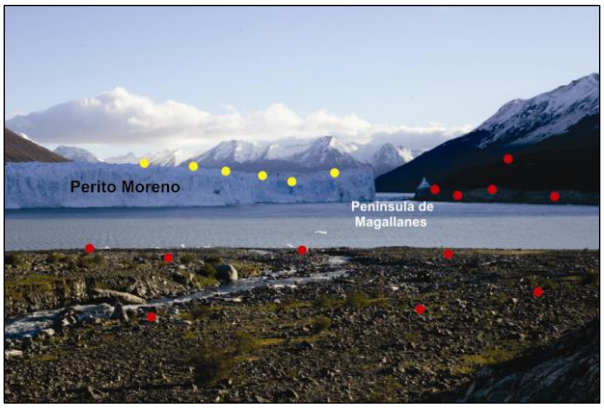

Figure 3. GCPs (red color) and check points (yellow color) distributed along the image.

3.3 Images correction

The overall processing workflow is shown in Fig. 4. In a first stage, the spatial resolution was calculated assuming a horizontal plane. Considering the focal of 50 mm and the pixel size of 7.2 microns, the size of the pixels for distances of 1000, 1500 and 2000 m respectively were obtained which gave values of 0.14, 0.22 and 0.29 m. Even when the camera has stable and precisely known internal geometries the lens distortions affect the measurement through photogrammetry processes in magnitudes that increase as the distance from the cameras increases. The most common geometrical distortions are the radial and decentering lens distorsions in fewer amounts. The maximum radial distortion calculated in an area covered by one image near to the edges gave a pixel size of 0.47 m to a maximum distance of 2000 m. But our area of interest is confined close to the principal point in the right quadrant, so the distortion calculated for this area resulted negligible adding to this that our view is not oblique.

On the other hand, the winds, temperature, platform structure, etc., may have produced the camera shifts and/or movements during the operation. These movements are transferred into the image in feature extraction error and result complex to perform the registration. Also the different climatic conditions as radiation, snow cover, as well as the time of taking pictures (illumination) can cause effects that prevent the correct matching between the time series. The matching of correlation procedures has the task of identify conjugate points. In our case it is assumed that the camera should not have changed their orientation but to minimize the potential shift GCPs provided the information necessary to ensure the quality, as well as to solve the orientation of images. The use of GCPs is

important to obtain precise georeferencing and subsequently increasing the reliability of the images sequence in the reference frame.

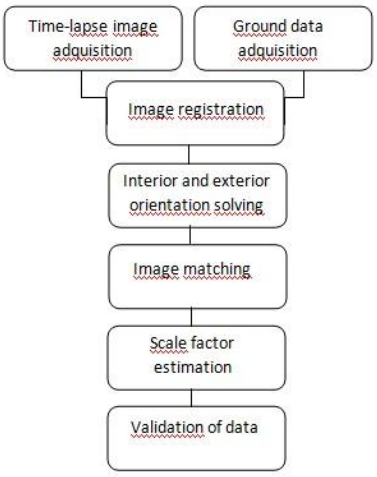

Figure 4. Workflow of the present study

Interior orientation does not mean only the calibrated focal length and the position of the principal point but also the coefficients of a polynomial to describe lens distortion (if the photo does not originate from a metric camera). If the camera position and orientation is unknown at least 3 GCPs on the object are necessary to compute the exterior orientation. Therefore, it was possible to work with only one camera due to the internal position data of the camera and the identification of features in the image conjugate. Thus, internal camera calibration parameters and coordinates of the projective center provide the necessary information. In this study, 12 GCPs were distributed on the image as was possible according to the topography (see Fig. 3). The points were projected into the Argentine GK2 local mapping frame allowed improving the image georeferencing, and the first image was used as a reference. To relate the sequence of images was used least squares matching and 2D affine transformation to map coordinates and correct the effects of camera movements. Tie points were measured to allow stronger correlation between the sequences, giving an RMS of 1.2 pixels. The uncertainty of the GCPs gave an RMS (Root mean squeare) of ± 30 m. This error is conjugated with the points that were taken by total station, which introduces considerable error in relation of measured by GPS.

The scale local error of any point depends on the distance between the surface of the glacier and the base of the camera. Positions and scale factor of checkpoints taken on the glacier surface at different depths were calculated, by assigning at each point the pixel of the camera image taking in account the angle represented for each pixel. The distances between the camera and the object were determined by intersection method. The difference in height (h1 - h0) obtained allowed to estimate the uncertainty on scale assignment. Given a maximum distance of 1800 m from the camera, in the area of the ice-dam collapse this value is 5% of the scale factor. For example a change in the water level in the lake of 10 m will have an error of 50 cm. Also, using the same method some object with known measures such as a boat were taking in account, but selecting a perpendicular view of the boat in the image respect to the axis of the camera. Finally, the calculations of displacements and velocities will be influenced by flow direction, in our case the direction is 45° respect to the camera axis. When we calculate the component conclude that the influence is despicable respect to the factor scale error.

3.4 Terrestrial validation

Water levels changes on the lake due to the increment occurring for the ice-dam were determined daily during the sequence studied. The sequence of images taken for the analysis include since October 1, 2012 until February 12, 2013, after the rupture of ice-damming. The images in greyscale were worked to optimize the assessment in the levels affected by weather, waves, ice, wind and lighting conditions on the images. The measurements were made by manual digitization in three different places over vertical outcrops. The final position of relative values was the mean height which dramatically reduces the error. We used a low-pass filter to minimize the noise in the different stages of the lake caused by the conditions stated above.

Data from images were correlated with daily data taken with a direct method on Lago Rico by Argentine Secretariat of Water Resources. The calculation of the Pearson *r* statistic (McKillup and Darby Dyar, 2010) provided the strength of a linear relationship for these two variables.

4. RESULTS

Levels of change in Lake Brazo Rico were detected. The relative difference height value in 135 days was 2.94 ± 0.07 m. Figure 4 shows the Brazo Rico lake and the water height level variations over this period. Black line show the trend of data taking by time lapse-photos (TL), the grey line is the trend by direct method (DM), and black dots line is the mean historical water level without influence of ice-dam during 1996-2001 and 2009-2011 period. Thus, the (TL) and (TM) data above the mean dot line means the water storage by the ice-dam.

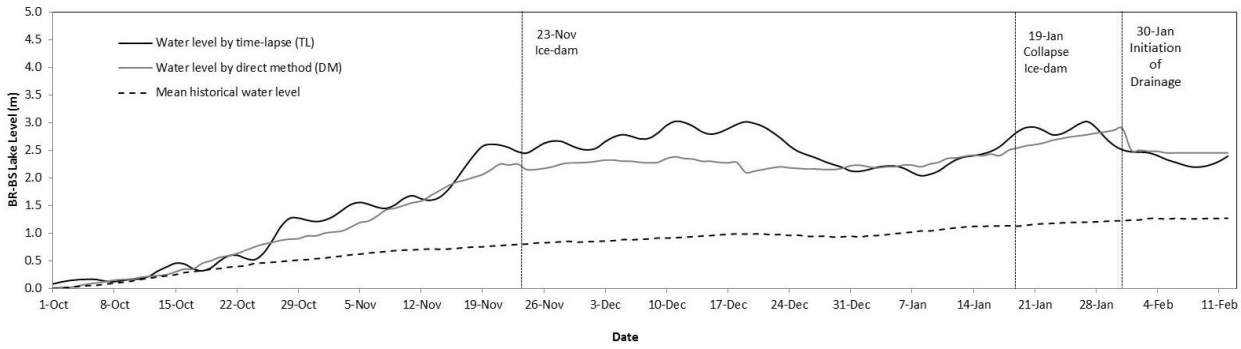

Figure 4. Water level trend of data taking by time lapse, direct method and mean water level without influence of ice-dam.

The tunnel started in the ice-dam on 23th November where it is observed that still filling of the dam. The data trend has upward tendency even when the dam breaks on January 19. The peak of maximum height level is found 11 days later, on January 29. On January 30 where a fall of -0.50 m is denoted that is related with the discharge of the dam. The lake drained completely in February.

The TL (black color) data were related with DM (grey color) as shown in Figure 4. Figure 5 show the correlation of the trend by Pearson coefficient. The variables have been converted to their Z scores, and indicate the strength relationship between them. Where $Z=\frac{Xi-\mu}{\sigma}$, and Xi a set of data; μ a mean value and σ is the standard deviation. The Z scores increase together along a straight line. Consequently, the value obtained for r = 0.96, and have a mean of -0.009 and standard deviation of 1.004 that means a good match agreement between both variables.

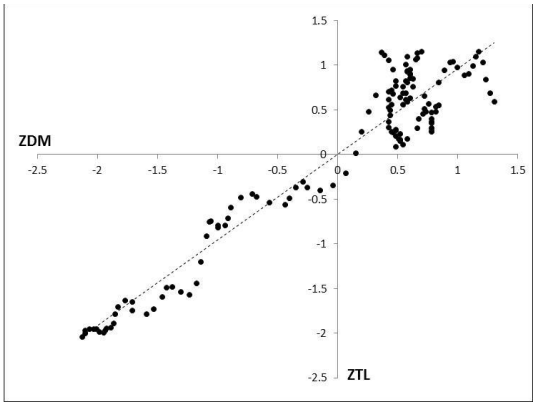

Figure 5. Distribution of TL and TM variables transformation (Z)

Ice-dammed lakes often exhibit temporary changes in behaviour drainage as shown in Figure 4, generally in response to fluctuations of glaciers (Tweed & Russel, 1999), initiating a discharge of water when the lake exceeds a critical threshold (Paterson, 1994), depending on the topography of the lake basin and the characteristics of the ice dam. This implies that a given drainage initiation mechanism may prevail in one place and not in another (Tweed & Russel, 1999).

The changes in width and height of the tunnel since November, 29 until it finally collapses in January, 19 were studied twice per day as shown in Figure 6. The tunnel corresponds to an ellipse of varying shape, where the glacier undergoes extra compression so the shape is not symmetric. At the beginning the tunnel has a minimum height value of 5.2 m and 21.5 m of width. After three days the trend of height data has almost constant variations with a tiny negative tendency until three days before the collapse that reach a maximum value of 22.3 m. This tendency is related by flattening in the upper part of the arc due to the tensions and forces of the glacier on the tunnel. Therefore, the width has a light positive tendency to reach a maximum value of 54.5 m that is related by the lateral undermining. After that the tunnel became shorter and then increases rapidly until broken.

O the other hand, the height variations of the front were obtained, near to the tunnel zone. The Figure 7 shows the information extracted from daily data during a sequence of 113 images. The mean height of the glacier in front damming area is 75 m. The evolution of the positions 1, 2, 3 (Figure 7a) shows the different effect that occur when the glacier moves towards to Peninsula de Magallanes. Position 1, has a very important feature with a mean advanced value of 47.15 md^{-1} ± 2.35 m, since it has the greatest suffers calving effect and it can be shown in each of the fractures occurs almost equidistant along the path. The mean velocity was of -0.10 md^{-1} ± 0.005 m. Position 2 and 3 has almost the same behaviour in the trend described a front advance with a mean velocity of 0.58 md^{-1} ± 0.03 m and 0.67 md^{-1} ± 0.003 m respectively This result is according to Ciappa et al. (2010) by cross correlation SAR imagery for the same period in 2009. The velocities are shown in Figure 7b,c,d and are the daily instant velocity of Positions 1,2 and 3. The values show sudden peaks associated to the calving effect and a big increment occur when the ice-dam collapse. The Figure 7e shows the height variation of the observed data. The evolution shows drastic changes experienced due to the release of calving. The peaks in a higher

position had a height of 86.99 md^{-1} ± 4.35 m that was reached due the retreat experience, in some cases with an average up to 10 m.

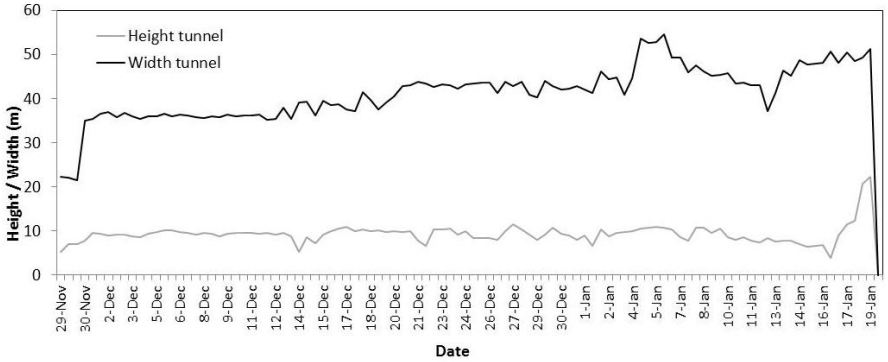

Figure 6. Height and width evolution of the tunnel.

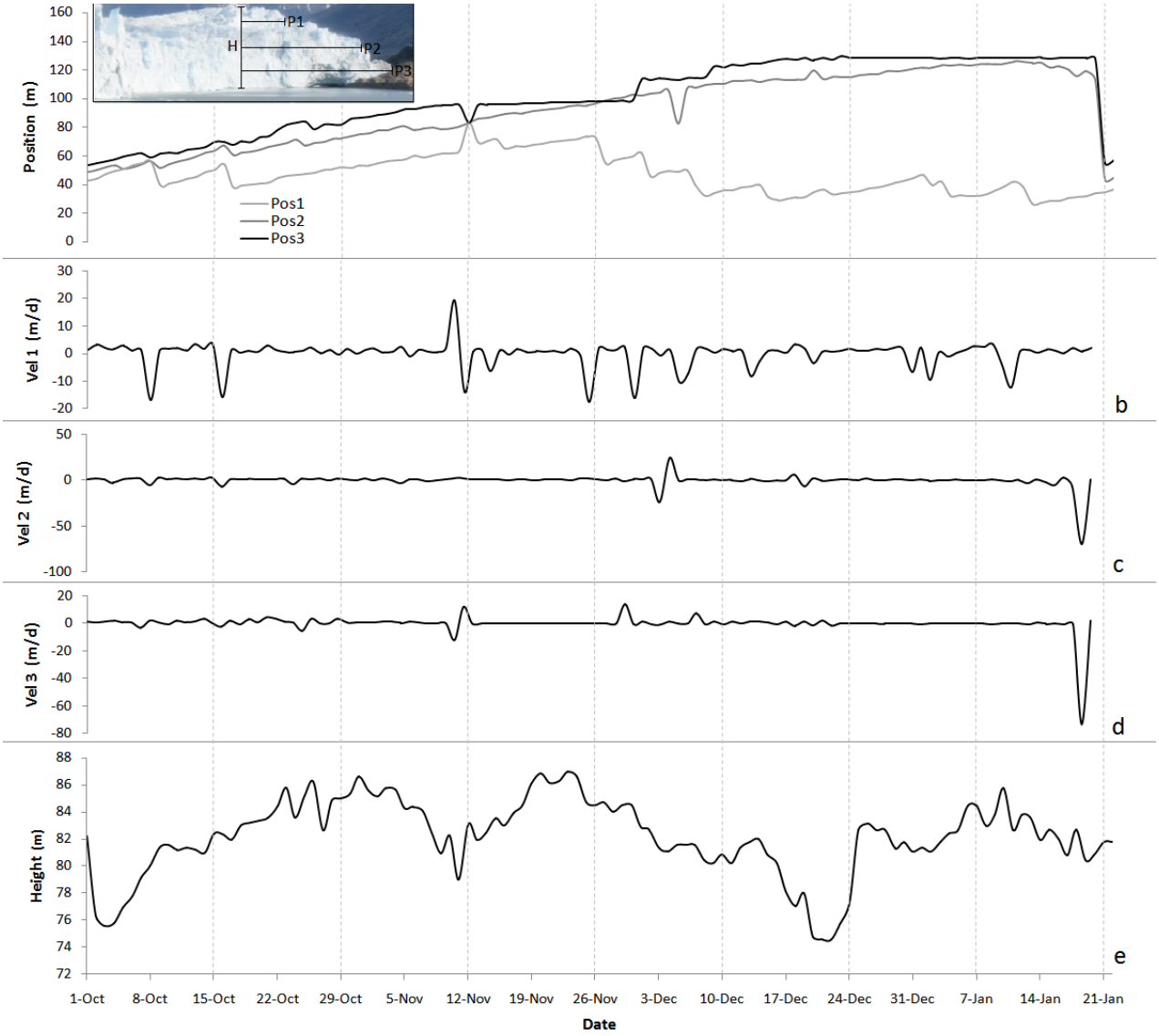

Figure 7. a). Evolution of the position 1, 2 and 3. b, c and d). Velocities of the position 1, 2 and 3. e). Height (H) evolution of the Perito Moreno front.

Conclusions

Time lapse terrestrial photogrammetry processes is a good technique to generate detail data in specific zone of glaciers and has the advantages in the monitoring with a good temporal resolution. This study demonstrates that image sequence acquisition from time-lapse photos can help to understand the behaviour and dynamics of glaciers such as Perito Moreno. The proposed technique produced acceptable results in the ice-dam evolution and estimation of elevation and planimetric changes, which cannot be observed effectively and rapidly with conventional methods. The validation in water level height changes gave a good match between TL and DM data. Also, result important complement and validate with another techniques such as satellite photogrammetry, LiDAR or SAR to compare model velocities among others. In future work, the authors will improve the image processing adding another camera in stereo model, and will propose an ice-dammed drainage triggers model in order to estimate the mechanism of the collapse produced in this glacier.

Acknowledgements: The authors would like to thank Pedro Skvarca for his advice and Adalberto Ferlito for field assistance. Robert Smalley Jr. (Univ. of Memphis, USA) provided the PS GNSS data. Parque Nacional Los Glaciares provided support in the area. Fieldwork was funded by grant PICT 2921-2012, Agencia Nacional de Ciencia y Tecnología Argentina (ANCyT)

REFERENCES

Ahn, Y. & Box J. E., 2010. Instruments and Methods. Glacier velocities from time-lapse photos: technique development and first results from the Extreme Ice Survey Greenland. Journal of Glaciology, 56: 198.

Aniya, M. and Skvarca, P., 1992. Characteristics and variations of Upsala and Moreno glaciers, southern Patagonia," Bulletin of Glacier Research, 10: 39-53.

Aniya, M., Sato, H., Naruse, R,. Skvarca, P., and Casassa, G., 1996. Remote sensing application to inventorying glaciers in a large, remote area-Southern Patagonia Icefield. Photogrammetric Engineering and Remote Sensing, 62: 1361-1369.

Ciappa, A., Pietranera, L., and Battazza, F., 2010. Perito Moreno Glacier (Argentina) flow estimation by COSMO SkyMed sequence of high-resolution SAR-X imagery, Remote Sens. Environ., 114(9): 2088–2096.

Dach, R., Hugentobler U., Fridez P., and Meindl M., 2007. BERNESE GPS Software Version 5.0. Astronomical Institute, University of Bern, Berna.

Danielson, B. and Sharp, M., 2013. Development and application of a time-lapse photograph analysis method to investigate the link between tidewater glacier flow variations and supraglacial lake drainage events. Journal of Glaciology 59: 287-302.

Harrison, W.D., K.A. Echelmeyer, D.M. Cosgrove and C.F. Raymond. 1992. The determination of glacier speed by time-lapse photography under unfavourable conditions. Journal of Glaciology, 38(129): 257–265.

Lauria, E.A., 2009: República Argentina–Adopción del Nuevo Marco de Referencia Geodésico Nacional POSGAR 07–RAMSAC. Novena Conferencia Cartográfica Regional de las Naciones Unidas para América, United Nations E/CONF.99/CRP.9, New York, 10–14 August.

McKillup and Darby Dyar, 2010. Geostatistics Explained An Introductory Guide for Earth Scientists. pp389.

Maas H.G., Casassa G., Schneider D, Schwalbe E, and Wendt A., 2010. Photogrammetric determination of spatio-temporal velocity fields at Glaciar San Rafael in the Northern Patagonian Icefield. The Cryosphere Discussions. 4, 2415–2432.

Paterson, W., 1994. The Physics of Glaciers. 2nd Edition. Pergamon Press. Oxford, New Cork, Seoul y Tokio, pp 385.

Rivera, A., Corripio, J., Bravo, C., and Cisternas, S., 2012. Glaciar Jorge Montt dynamics derived from photos obtained by fixed cameras and satellite image feature tracking, Annals of Glaciology, 53: 60A152.

Svanem, M., 2010. Terrestrial Photogrammetry for velocity measurements of Kroneebreen calving front . Master Thesis, Norwegian University of Life Sciences.

Takeshi Hashimoto, Mitsuo Kaneko, András Rövid, Shinji Isono, Tomoyuki Sone, Kazushige Baba, Akira Fukuda, Masamu Aniya, Nozomu Naito, Hiroyuki Enomoto, Pedro Skvarca, 2009. An introduction of high-recise 3D measurement system and its applications. Journal of Automation, Mobile Robotics & Intelligent Systems, 3: 4.

Tweed, F. & Russel, A., 1999. Controls on the formation and sudden drainage of glaciar-impounded lakes: implications for jökulhlaup characteristics. Progress in Physical Geography, 23 (1): 79-110.